Chemical Engineering Journal 104 (2004) 35–43

Chemical Engineering Journal

www.elsevier.com/locate/cej

Modeling of counter current moving bed gas-solid reactor used in direct reduction of iron ore

Daniel R. Parisi*, Miguel A. Laborde

Departamento de Ingeniería Química, Facultad de Ingeniería, Universidad de Buenos Aires, Pabellón de Industrias, Ciudad Universitaria, 1428 Buenos Aires, Argentina

Received 11 November 2003; received in revised form 6 August 2004; accepted 9 August 2004

Abstract

In this work, the shaft furnace reactor of the MIDREX® process is simulated. This is a counter current gas-solid reactor, which transforms iron ore pellets into sponge iron.

Simultaneous mass and energy balance along the reactor leads to a set of ordinary differential equation with two points boundary conditions. The iron ore reduction kinetics was modelated with the unreacted shrinking core model. Solving the ODE system allows to know the concentration and temperature profiles of all species within the reactor.

The model was able to satisfactorily reproduce the data of two MIDREX® plants: Siderca (ARGENTINA) and Gilmore Steel Corporation (U.S.A.). Also, it was used to explore the performance of the reactor under different operating conditions. This capacity could be used for design and control purpose.

Keywords: Shaft furnace simulation; Gas-solid reactor; Moving bed; Direct reduction.

1. Introduction

Direct reduction of iron ore is today's major process for generating metallic iron, necessary in the iron and steel industry. World production of direct reduce iron (DRI) has grown from near zero in 1970 to 45.1 Mt in 2002. MIDREX® Technology is the most important one, responsible for the 66.6% of the world total DRI production. Its main reactor (the shaft furnace) is a moving bed reactor.

The first studies related to moving bed solid-gas reactors were performed by Munro and Amundson [1], Amundson [2] and Siegmund et al. [3]. In these works, the authors used a linear function of the solid temperature in order to approximate the reaction rate and to obtain analytical solutions. The validity of this solution is limited to a narrow range of temperatures.

Schaefer et al. [4] studied the heat generation in a steady-state reactor. They used a step function for the heat balance and the results show the existence of multiplicity of steady-states.

Yoon et al. [5] developed a model for a Lurgi type reactor used in the carbon gasification. They considered the same temperature in both phases (solid and gas) and the shrinking unreacted core model for the solid particle.

Amundson and Arri [6] analyzed the same system but considering different temperatures in both phases.

Arce et al. [7] studied a countercurrent moving bed reactor using a heterogeneous model for the reactor design and the shrinking core model for the solid particle. They applied both models to an irreversible first order exothermic reaction.

Rao and Pichestapong [8] developed a model for a reactor in which the reduction of iron mineral is carried out. The model considers that the controlling step is the mass transfer of the gaseous reactants in the product solid layer. The concentration of the gaseous species on the interface gas-solid is that of the equilibrium and it was evaluated using an iterative

* Corresponding author. Tel.: +54 11 4576 3240; fax: +54 11 4576 3241.
E-mail addresses: parisi@di.fcen.uba.ar (D.R. Parisi), miguel@di.fcen.uba.ar (M.A. Laborde).

1385-8947/$ – see front matter © 2004 Elsevier B.V. All rights reserved.
doi:10.1016/j.cej.2004.08.001

Nomenclature

A_p	pellet external area (cm^2)
C	reactor gas concentration (mol/cm^3)
D	effective diffusion coefficient (cm^2/s)
G_m	molar flow ($mol/cm^2\ s$)
H	reaction enthalpy (cal/mol)
h	global heat transfer coefficient (pellets/gas) ($cal/s/cm^2/K$)
k	kinetics constant of the surface reaction (cm/s)
k_g	external mass transfer coefficient (cm/s)
L	reduction zone length (cm)
M_w	molecular weight
n_p	number of pellets per unit volume ($1/cm^3$)
R	reaction rate ($mol/cm^3 s$)
$\hat{R}$	reaction rate per pellet (mol/s)
r_0	external radius of the pellet (cm)
r_c	radius of the unreacted core (cm)
T	temperature (°C)
u	gas velocity (cm/s)
X	extent of reaction/extent of reactant conversion (mol/cm^3)
z	space variable inside the reactor (cm)

Subscripts

atm	atmosphere
i	ith reaction
in	reactor inlet
j	jth reactant (gas or solid)
n	gaseous reactant
rs	reactive solid (Fe_2O_3)
ps	product solid (Fe)
sol	solid
g	gas

Greek letters

α	stoichiometric coefficient
ρ	density of the solid reactant (g/cm^3)

method. As a consequence, the problem cannot be solved in terms of differential equations system. In this paper, the heat balance is avoided since the authors assumed a linear function of the temperature with the reactor length.

The aim of this work is to model and simulate a solid-gas countercurrent moving bed reactor in which the reduction of iron ore pellets is performed using CO and H_2 as reducing gases.

In order to do that, mass and energy balance are taken into account simultaneously. This leads to a set of ordinary differential equation with two point boundary conditions.

The model is validated with data from two industrial plants. Also, it is used to explore the performance of the reactor under different operating conditions.

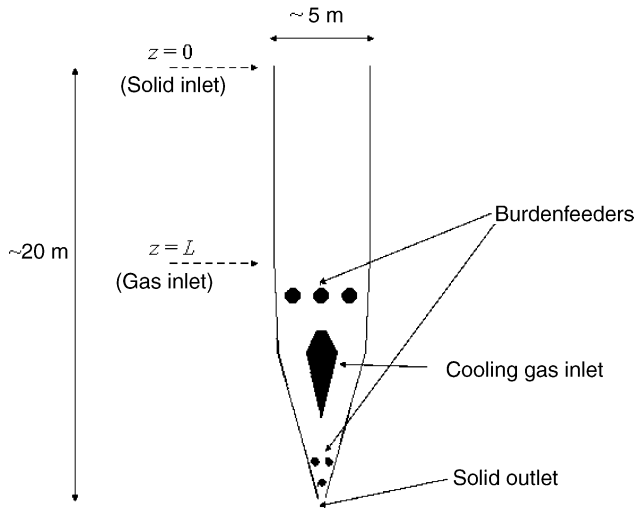

Fig. 1. Shaft furnace geometry.

1.1. Shaft furnace of the MIDREX® process

The main function of the shaft furnace is to generate sponge iron from iron ore. The solids flow downwards by gravity and the reducing gases flow upwards in counter current, while the corresponding chemical transformations occur. Fig. 1 shows a scheme of the reactor.

As it can be observed, the furnace consists of a vertical cylindrical container, with a conic lower zone. The inner wall is covered with insulating materials resistant to erosion.

The reducing gases enter by the middle zone of the reactor through the bustle, which consists of a channel with approximately 70 nozzles that direct the gas towards the center of the solid bed.

Immediately underneath, the upper burdenfeeders are located. Following in descendent order one can found: the wind boxes (which take the cooling gas that circulates around the lower conical zone of the reactor), cooling gas distributor or ("inverted Christmas tree"), which besides to inject cooling gases has the function to support most of the bed weight.

Gases going out from the shaft furnace are recycled into another reactor: the Reformer. This is a fixed bed catalytic reactor, which transforms the process gas (with addition of natural gas) into reducing gas again.

2. The model

In order to model the MIDREX® shaft furnace, the following approximations are considered:

(a) The iron ore pellet consumption is governed by the unreacted shrinking core model. This aproximation was made by several authors, see for instance [8,9].
(b) Mass and heat transfer resistances through the film around the solid particle are negligible comparing with

diffusional resistance inside the porous solid ($k_g \gg D/2/r_0$).

(c) Only steady-state operating conditions will be considered.

(d) Plug flow is assumed for gas and solid phase.

Due to high gas flow rate in the reactor, turbulence regime is reached. Under this situation, inertial effects are predominanant. So it will not be considered neither axial nor radial dispersion [10].

For the solid phase this hypothesis was verified through a previous work [11]. Distinct element method simulations (DEM) were performed in order to study the granular bed dynamics of a typical MIDREX® shaft furnace.

Only the global direct reduction reactions are taken into account. The area of interest is the reduction zone of the reactor. Carburization reaction will not be considered as they occur in the lower zone.

The reaction system studied is the following:

$$\tfrac{1}{3}Fe_2O_3\,(s) + H_2\,(g) = \tfrac{2}{3}Fe\,(s) + H_2O\,(g) \quad (R1)$$

$$\tfrac{1}{3}Fe_2O_3\,(s) + CO\,(g) = \tfrac{2}{3}Fe\,(s) + CO_2\,(g) \quad (R2)$$

It must be noted that the water gas shift reaction (WGSR) is a linearly dependent reaction with reactions R1 and R2 (In fact, R1 − R2 = WGSR). The WGSR is a very important reaction in the reductor reactor studied. So even it was not chosen as one of the linearly independent reactions of the system, it is taken into account implicitly, in the present analysis.

The extent of reaction is defined in terms of concentration as:

$$C_j = C_j^0 + \sum_i \alpha_j^i X_i \quad (1)$$

for each species j and where α_j^i is the stoichiometric coefficient.

From definition (1), it can be wrote for the gaseous phase,

$$X_1 = C_{H_2}^0 - C_{H_2} \quad (2)$$

$$X_2 = C_{CO}^0 - C_{CO} \quad (3)$$

and for the solid phase,

$$X_{rs} = X_1 + X_2 = 3(C_{Fe_2O_3}^0 - C_{Fe_2O_3}) \equiv X_3 \quad (4)$$

Considering the unreacted shrinking core model and that the concentration of reactive solid must be measured per unit of reactor volume, it is possible to relate the radius of the unreacted core (r_c) with the solid conversion (X_3) through Eq. (5),

$$r_c = \left(r_0^3 - \frac{X_3\, M_w}{n_p 4\pi\rho}\right)^{1/3} \quad (5)$$

where r_0 is the external radius of the pellet, n_p the number of pellets per unit reactor volume, M_w and ρ are the molecular weight and the density of the reactive solid, respectively.

The origin of coordinates is placed at the top of the reactor (see Fig. 1).

Under the above assumptions (a)–(d), the mass and energy balances for a steady-state counter current moving bed reactor can be stated as:

- Gas phase

$$u\frac{dX_1}{dz} + n_p\hat{R}_1(X_1, X_3) = 0 \quad (6)$$

$$u\frac{dX_2}{dz} + n_p\hat{R}_2(X_2, X_3) = 0 \quad (7)$$

$$\frac{dT_g}{dz} - \frac{n_p A_p h(T_{sol} - T_g)}{G_{m_g} C_{p_g}(X_1, X_2, T_g)} = 0 \quad (8)$$

- Solid phase

$$u_{sol}\frac{dX_3}{dz} + n_p(\hat{R}_1(X_1, X_3) + \hat{R}_2(X_2, X_3)) = 0 \quad (9)$$

$$\frac{dT_{sol}}{dz} - \frac{n_p}{G_{m_{sol}}(X_3) C_{p_{sol}}(X_3, T_{sol})} \times \left[A_p h(T_{sol} - T_g) - \sum_i \Delta H_i(T_{sol})\hat{R}_i(X_i, X_3, T_{sol})\right] = 0 \quad (10)$$

with the following boundary conditions:

$$X_1(z = L) = 0, \qquad X_2(z = L) = 0,$$
$$X_3(z = 0) = 0, \qquad T_g(z = L) = T_g^{in},$$
$$T_s(z = 0) = T_{atm} \quad (11)$$

The problem is solved making an attempt to predict X_1, X_2 and T_g at $z = 0$ (shaft furnace gas outlet) so that after solving the equations system (6)–(10) the boundary conditions at $z = L$ are satisfied, $X_1(z = L) = X_2(z = L) = 0$ y $T_g(z = L) = T_g^{in}$.

The shrinking core model is used for the solid pellet; the corresponding reaction rate expression per pellet is given by:

$$\hat{R} = \frac{-4\pi r_c^2 C_n}{(1/k_n + r_c/D_n - r_c^2/r_0 D_n)} \quad (12)$$

where n = 1,2 denotes H_2 and CO, respectively. The reaction rate per unit volume of reactor (R) is obtain through

$$R = n_p\hat{R} \quad (13)$$

It must be noted that this model is based on an irreversible kinetics, which limits the validity of the simulation in the situations in which the gas composition is far from equilibrium.

The solid molar flow ($G_{m_{sol}}$) is a function of X_3, related to shrinking core radius by Eq. (5), such as $G_{m_{sol}}$ can be evaluated using expression (14):

$$G_{m_{sol}}(r_c) = G_{m_{sol}}^L \frac{[1/2\, {r_c}^3\rho_{rs}/M_{w_{rs}} + ({r_0}^3 - {r_c}^3)\rho_{ps}/M_{w_{ps}}]}{[{r_c}^3\rho_{rs}/M_{w_{rs}} + ({r_0}^3 - {r_c}^3)\rho_{ps}/M_{w_{ps}}]} \quad (14)$$

The solid specific heat was calculated using:

$$C_{p_s} = \frac{[c_p^{rs}\rho_{rs}{r_c}^3 + c_p^{ps}\rho_{ps}(r_0^3 - r_c^3)]}{[\rho_{rs}r_c^3 + \rho_{ps}(r_0^3 - r_c^3)]} \quad (15)$$

This expression considers the C_p weighted average of reactive solid (rs) and product solid (ps) for any state of transformation given by the unreacted radius (r_c). Heat transfer coefficient (h) is obtained from Chilton and Colburn correlation, used for fixed bed reactors (neglecting the resistance in the gaseous film),

$$h = \frac{1}{\langle C_p \rangle G_{m_g}} Pr^{2/3} \quad (16)$$

where Pr is the Prandtl number.

Values of reaction enthalpies (ΔH) and specific heats (C_p) were taken from NIST (http://webbook.nist.gov/chemistry/).

The kinetics and diffusion parameters take as reference those that were obtained from experiments performed in a laboratory gas-solid fixed bed reactor [12] at 900 °C with SAMARCO pellets.

Kinetics coefficients follow Arrhenius law. Activation energies were obtained from literature. For the R1 reaction, $E_{a_1}/R_g = -179.14$ corresponding to McKewan [13] and for the reaction R2, $E_{a_2}/R_g = -342.43$ reported by Bohnenkamp and Riecke [14].

Pre-exponential values were fitted using the available plant data in each case, depending on the different types of pellets.

The dependency of the effective diffusion coefficients with temperature is taken as $D_i \sim T^{1.75}$ [15].

The differential equations system (6)–(10) with boundary conditions (11) is solved numerically using an explicit Runge–Kutta method based on the Dormand–Prince pair [16].

3. Results and discussion

The model was validated comparing the estimated values with values of exit gas composition and metallization level of two MIDREX® plants: Siderca (Campana, Buenos Aires, Argentina) and Gilmore Steel Corporation (Portland, Oregon, U.S.A.).

3.1. Siderca MIDREX® plant

In this section the model will be used to simulate the reduction zone of the shaft furnace belonging to Siderca plant in Campana, Buenos Aires, Argentina.

Table 1 summarizes the operating conditions recorder during 2 h of an arbitrary day.

The values of kinetics constants, diffusion coefficients and heat transfer coefficient (h) used in the simulation are shown in Table 2.

With the values and operating conditions given in Tables 1 and 2, the differential equations system (6)–(10) was solved numerically obtaining the profiles shown in Figs. 2 and 3.

Table 1
Operating conditions of Siderca plant

Gas	
Gas flow rate	1 40 000 Nm^3/h
Inlet composition (at $z = L$)	
H_2	52.9%
CO	34.7%
H_2O	5.17%
CO_2	2.47%
$CH_4 + N_2$	4.65%
Inlet temperature	957 °C (1230 K)
Solid	
Production (Fe)	100 t/h
Mineral pellet density	3.4 g/cm^3
Sponge iron density	3.1 g/cm^3
Pellet ratio (r_0)	0.5 cm
n_p	0.99 pellets/cm^3
Reactor	
Reaction zone length	1000 cm
Diameter	488 cm

It can be seen that the two extents of reaction are very similar, in the same way as reaction rates even when the H_2 concentration is greater than that of CO. This indicates that the different concentrations used in the reducing gas allow that both reducing gases act simultaneously throughout the entire reactor, removing the same amounts of oxygen. Also it is clear that the CO is a better reducer than the H_2 since with smaller concentrations of CO similar reaction rates are achieved.

The fact that reaction rate R2 is greater than R1 near the gases outlet (low temperature) is a consequence of the activation energies values (E_{a_2} is two times greater than E_{a_1}). This causes that the difference between both reaction rates is more sensible to the temperature than to the concentrations.

In the same Fig. 2, it can also be appreciated that molar fractions of gases (reactive and products) evolve monotonically within the reactor, and that the temperatures of the gases and solids tend to be uniform as z grows.

Fig. 3 shows that the whole reactor length is used efficiently for the transformation of the solid, which in fact is incomplete (94% of metallization). This situation is preferable to one in which the solid is transformed completely before arriving to the solid outlet, in this case, the residence time would be greater than the necessary and the production would be lower than the maximum production capacity of the plant.

Table 2
Kinetics constants, effective diffusion coefficients and heat transfer coefficient used in the simulation of the Siderca shaft furnace

k_1	$0.225 \exp(-14700/82.06/T)$ cm/s
k_2	$0.650 \exp(-28100/82.06/T)$ cm/s
D_1	$1.467 \times 10^{-6} \times T^{1.75}$ cm^2/s
D_2	$3.828 \times 10^{-7} \times T^{1.75}$ cm^2/s
h	4×10^4 cal/cm^2/s/K

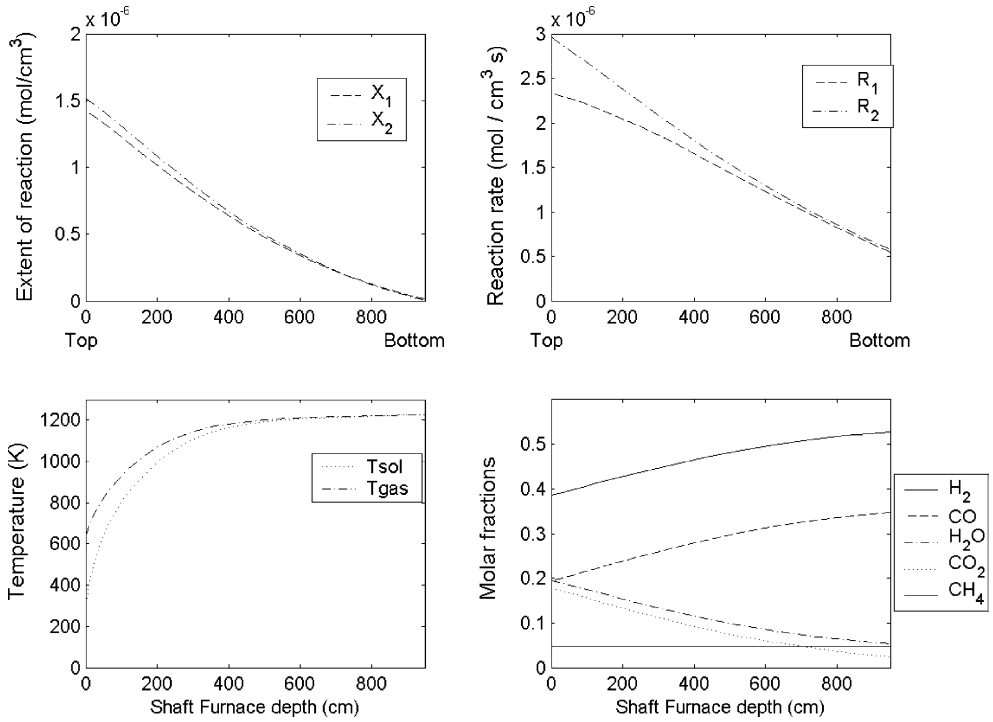

Fig. 2. Profiles of many variables along the reduction zone of the Siderca shaft furnace.

In addition, the simulation allows to predict the outlet composition of gases (at $z = 0$) as it is shown in Table 3.

Data from Table 3 was obtained directly from instruments in the plant. The predictions of the model agree satisfactorily with this data, within the experimental error.

3.2. *Gilmore MIDREX® plant*

Rao y Pichestapong [8] published data from another MIDREX® plant, the Gilmore Steel Corporation Plant in Portland, Oregon, U.S.A.

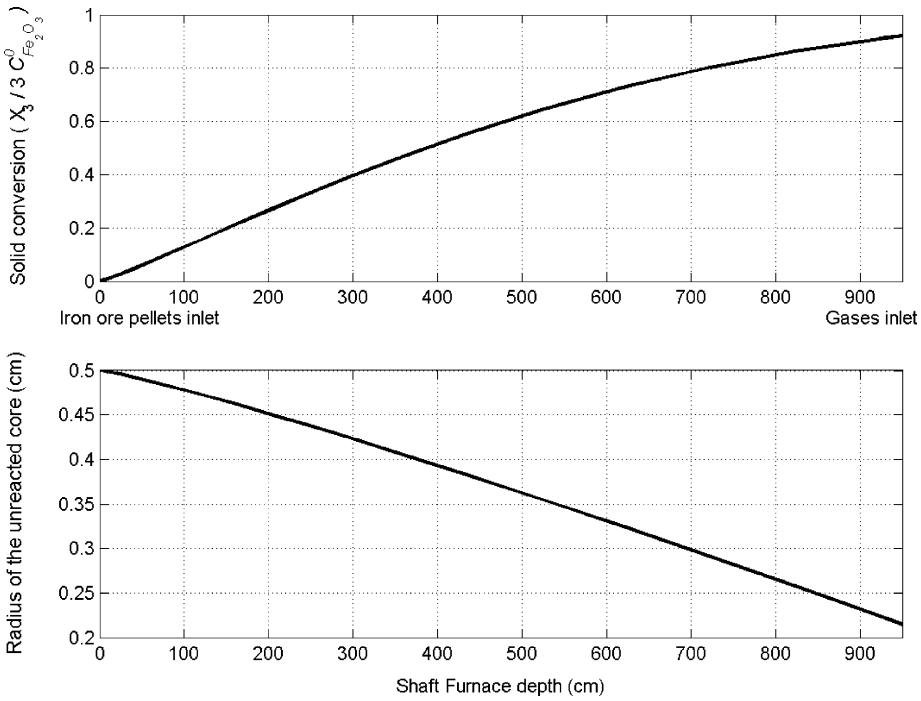

Fig. 3. Profiles of variables related to the solid phase along the reduction zone of the Siderca shaft furnace.

Table 3
Comparison of the Siderca Plant data with model predictions

	SIDERCA data (dry base) (%)	MODEL data (dry base) (%)
Outlet gas composition ($z = 0$)		
H_2	49.0 ± 2	48.19
CO	23.6 ± 1	24.15
H_2O	–	–
CO_2	21.3 ± 1.2	21.90
$CH_4 + N_2$	6.1 ± 0.8	5.76
Metallization	93.7 ± 1	93.8

Table 4
Operating conditions of gilmore plant

Gas	
Gas flow rate	53863 Nm^3/h
Inlet composition (at $z = L$)	
H_2	52.58%
CO	29.97%
H_2O	4.65%
CO_2	4.80%
$CH_4 + N_2$	8.10%
Pressure	1.4 atm
Solid	
Production (Fe)	26.4 t/h
Mineral pellet density	4.7 g/cm^3
Sponge iron density	3.2 g/cm^3
Pellet ratio (r_0)	0.55 cm
n_p	0.64 pellets/cm^3
Reactor	
Reaction zone length	975 cm
Reactor diameter	426 cm

The model was also applied to this plant. The operating conditions are shown in Table 4.

Regarding the gas flow rate per ton of sponge iron produced, it can be noted that these operating conditions are less efficient that those of Siderca.

This difference is due to, at least, two factors. First, the apparent density of iron ore pellets is greater in the case of Gilmore Plant. Second, the concentration of CO in the reducing gas is lower.

As in the previous section the differential equations system (6)–(10) was solved numerically, but with the values and operating conditions given in Tables 4 and 5

These values are similar to those in Table 2. The kinetics and effective diffusive parameters were adjusted in order to fit the plant data. A natural reason for this difference is that the type of pellet and the operating conditions are different.

Table 5
Kinetics constants, effective diffusion coefficients and heat transfer coefficient used in the simulation of the Gilmore shaft furnace.

k_1	$0.114 \exp(-14700/82.06/T)$ cm/s
k_2	$0.283 \exp(-28100/82.06/T)$ cm/s
D_1	$1.467 \times 10^{-6} \times T^{1.75}$ cm^2/s
D_2	$1.276 \times 10^{-7} \times T^{1.75}$ cm^2/s
h	1×10^{-4} cal/cm^2/s/K

Table 6
Comparison of gilmore data with model predictions

	GILMORE data (%)	MODEL data (%)
Outlet gas composition ($z = 0$)		
H_2	37.0	36.7
CO	18.9	18.5
H_2O	21.2	20.5
CO_2	14.3	16.1
$CH_4 + N_2$	8.6	8.2
Metallization ($z = L$)	93	92.8

The coefficient h was calculated from Eq. (16).

Fig. 4 shows the evolution of several variables along the reaction zone of the shaft furnace. In this case (D_2 is lower than in the previous case and there are different operating conditions) it can be observed that the reaction rate R1 is smaller than R2 near to the gases outlet ($z = 0$), where iron ore pellets are fresh ($r_c \approx r_0$) because the pre-exponential factor k_{02} is greater than k_{01}.

However, when r_c begins to be small, the reaction rate is controlled by the diffusional resistance in the ash layer and, in consequence, R2 results lower than R1.

In Table 6 the model prediction of the Gilmore plant data [8] are compared.

Also in this case the model reproduced the data satisfactorily.

4. Analysis of alternative operating conditions

In this section the model will be used to simulate the behavior of the Siderca shaft furnace in extreme operating conditions that are not used normally.

4.1. Production versus metallization

The relation between the production and the conversion of the solid, assuming the same composition and flow rate of the reducing gas (Table 1), is analyzed.

To maintain constant the composition of gases while varying the production is not a simple task, due to the recirculation that exist between the shaft furnace and the reformer, which produces the reducing gases. For that reason, it must be clear that the validity of this study is limited to the hypothetical case in which the same characteristics of the reducing gas can be maintained.

If it is desired to increase the metallization, the residence time of pellets inside the reactor must be increased. But this would decrease the production. Alternatively, if the production increases the metallization decreases.

Results of the simulations varying the wished production are shown in Table 7.

It can be observed that if a complete metallization is reached, the production would be lower by a 30% (70 t/h). Also if the production increases, the metallization level would fall bellow the level required by the steel mill (92%).

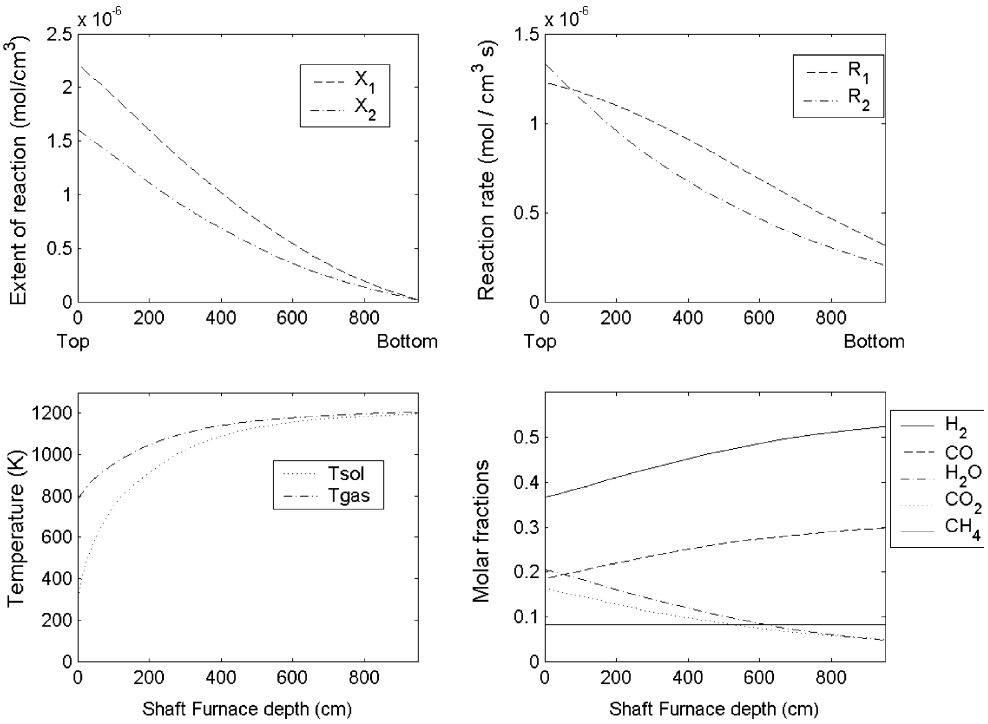

Fig. 4. Profiles of many variables along the reduction zone of the Gilmore shaft furnace.

Table 7
Variation of the metallization for different productions. The flow rate and the composition of the reducing gas are those of Table 1

Production Fe (t/h)	Metallization (%)
50	100
70	100
80	99.2
90	97.5
100	93.8
110	91.5

In a normal operation, the plant produces 100 t/h with 94% of metallization (superior to the acceptable minimum of 92%). In this case, the whole reactor is used efficiently (see Fig. 3). Nevertheless, the production could be slightly increased before reaching a metallization of 92%.

Fig. 5 shows the evolution of different variables within the reactor in the case in which the complete conversion of the solid is reached. This situation also serves to test the validity of the model when the chemical reactions stop because the solid was completely reduced.

It can be observed that beyond 6 m depth approximately, there is no chemical reaction because the solid is already reduced. The reaction takes place near the entrance of the solid and the exit of gases.

4.2. Increase of CO in the reducing gas

As it has been said, the carbon monoxide is a better reducer than hydrogen. Consequently some simulations are performed varying the relation H_2/CO. This allows analyzing the influences of that relation over the iron production.

Concentration of both reducing gases in the feed is 87.6% (Siderca plant, Table 1). The percentage of each reducing specie (CO and H_2) will be varied so that their sum remains constant (87.6%). Molar flows of the other species are not varied. Then we explore how much it is possible to increase the production (maintaining a metallization of 94%) as the proportion of CO increases. Table 8 shows the results of simulations.

It is observed, indeed, that when the proportion of CO is increased with respect to the H_2, the model predicts a production increment of approximately 7% between the extreme values studied.

Naturally, the operating conditions of the Reformer reactor (the other main reactor of MIDREX® process which provides the reducing gases) should be changed in order to obtain the desired H_2/CO ratio. But for doing this, it is necessary a coupled analysis of both reactors simultaneously. Besides, limitations at the reformer could arise to achieve the studied values.

Table 8
Predicted effect of the CO/H_2 relation (in the composition of the reducing gas) over the production of sponge iron in the MIDREX® process

CO% (at $z = L$, gas inlet)	H_2% (at $z = L$, gas inlet)	Sponge iron production (t/h)
34.7	52.9	100
40.0	47.6	104
43.8	43.8	107

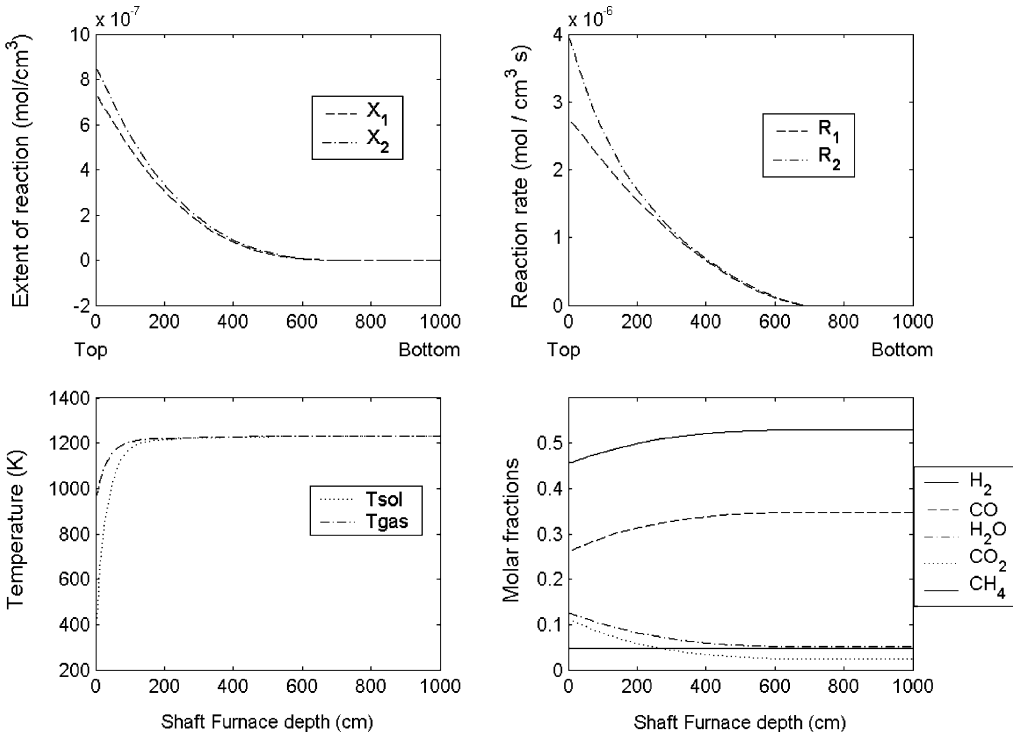

Fig. 5. Profiles of different variables along the reduction zone of the Siderca shaft furnace with a production of 50 t/h.

5. Conclusions

The reduction zone of the shaft furnace of the MIDREX® direct reduction process was simulated. In order to do this, mass and energy balances were solved for each phase in the countercurrent gas-solid reactor. The resolution of the differential equations system allows knowing the evolution of several variables throughout the reactor.

The model satisfactorily fit the data from at least two MIDREX® plants (Siderca SA in Argentina and Gilmore Steel Co. in the U.S.). In addition, they allow exploring the behavior of the reactor for different operating conditions. This could become an important tool for controlling and modifying the shaft furnace operating conditions.

The kinetics used in the simulations were found in a laboratory scale reactor described in [12]. Also some parameters were slightly adjusted for both different plants in order to fit the avaible plant data and taking into account the different type of iron ore pellets and operation conditions.

The proposed model allowed studying abnormal operation regimes, for example the relation between metallization and production of iron and how the production is affected by the proportion of carbon monoxide used in the reducing gas.

With respect to metallization, it is observed that if it would increase to 100% (gain of 6% in metallization), the production must decrease to 70% (loose of 30% in production), which obviously, is not advisable. Therefore if the plant works in such form that the metallization level was around 94%, it would be close to the optimum.

Concerning the carbon monoxide, simulations predict that greater it is the CO proportion; greater it will be the production of iron (maintaining the total gas flow rate and the metallization level fixed). However, an optimization analysis on this subject must be done considering a coupled simulation of both reactors: the Shaft Furnace and the Reformer.

Acknowledgements

Authors would like to acknowledge to SIDERCA S.A. for the contribution of plant data, to Francisco Ajargo for useful comments and to José Comas for text revision.

References

[1] W.D. Munro, N.R. Amundson, Solid-fluid heat exchange in moving beds, Ind. Eng. Chem. 42 (1950) 1481.
[2] N.R. Amundson, Solid-fluid interactions in fixed and moving beds, Ind. Eng. Chem. 48 (1956) 26.
[3] C.W. Siegmund, W.D. Munro, N.R. Amundson, Solid-fluid interactions in fixed and moving beds. Two problems on moving beds, Ind. Eng. Chem. 48 (1956) 43.
[4] R.J. Schaefer, D. Vortmeyer, C.C. Watson, Steady state behaviour of moving bed reactors, Chem. Eng. Sci. 29 (1974) 119.
[5] H. Yoon, J. Wei, M.M. Denn, A model for moving bed coal gasification reactors, AIChE J. 24 (1978) 885.
[6] N.R. Amundson, L.E. Arri, Char gasification in counter current reactor, AIChE J. 24 (1978) 87.
[7] P.E. Arce, O.M. Alfano, L.E. Arri, Modelo heterogéneo de un reactor de lecho móvil, Rev. Latinoamericana de Transferencia de Calor y Materia 6 (3) (1982) 99–112.

[8] Y.K. Rao, P. Pichestapong, Modelling of the midrex direct-reduction iron making process: mass transfer and virtual equilibrium at steady state, in: XVth CMMI Congress, Johannesburg, SAIMM, 1994, pp. 81–92.
[9] E. Kawasaki, J. Sanscrainte, T.J. Walsh, AIChE J. 8 (1962) 48.
[10] C.P. La Singh, D.N. Saraf, Ind. Eng. Chem. Process Des. Dev. 18 (1979) 364.
[11] D.R. Parisi, S. Masson, J. Martinez, Partitioned DEM simulation of granular flow within industrial silos, J. Eng. Mech. ASCE 130 (7) (2004) 771–779.
[12] D.R. Parisi, M.C. Mariani, M.A. Laborde, Solving differential equations with unsupervised neural networks, Chem. Eng. Process. 42 (8–9) (2003) 715–721.
[13] W.M. McKewan, Trans. Metall. Soc. AIME 224 (1962) 2–5.
[14] K. Bohnenkamp, E. Riecke, Arch. Eisenhüttenwes 42 (1971).
[15] E.N. Fuller, P.D. Schettler, J.C. Giddings, Ind. Eng. Chem. 58 (5) (1966) 18–27.
[16] J.R. Dormand, P.J. Prince, A family of embedded Runge-Kutta formulae, J. Comp. Appl. Math. 6 (1980) 19.